Parity nonconservation for neutron resonances in ^{232}Th

C. M. Frankle,[1,*] J. D. Bowman,[2] J. E. Bush,[1,†] P. P. J. Delheij,[3] C. R. Gould,[1] D. G. Haase,[1] J. N. Knudson,[2] G. E. Mitchell,[1] S. Penttilä,[2] H. Postma,[4] N. R. Roberson,[5] S. J. Seestrom,[2] J. J. Szymanski,[2,‡] S. H. Yoo,[2] V. W. Yuan,[2] and X. Zhu[5,§]

(TRIPLE Collaboration)

[1]*North Carolina State University, Raleigh, North Carolina 27695*
and Triangle Universities Nuclear Laboratory, Durham, North Carolina 27706
[2]*Los Alamos National Laboratory, Los Alamos, New Mexico 87545*
[3]*TRIUMF, Vancouver, British Columbia, Canada V6T 2A3*
[4]*University of Technology, P.O. Box 5046, 2600 GA, Delft, The Netherlands*
[5]*Duke University, Durham, North Carolina 27706*
and Triangle Universities Nuclear Laboratory, Durham, North Carolina 27706

(Received 6 April 1992)

Parity nonconserving (PNC) longitudinal analyzing powers were measured for 23 p-wave neutron resonances in ^{232}Th. Seven resonances show effects of greater than 2.4σ statistical significance—the largest sample yet measured in a single nucleus. All seven analyzing powers have positive sign. Strong sign correlations are not a feature of the conventional statistical model of parity mixing between compound nuclear states. The asymmetry was expressed as a sum of two terms: a constant asymmetry and a fluctuating asymmetry. With this ansatz the root-mean-square PNC matrix element $M=1.2^{+0.5}_{-0.4}$ meV, which corresponds to a spreading width of $\Gamma^{PV}=6\times10^{-7}$ eV.

PACS number(s): 25.40.Ny, 24.80.Dc, 11.30.Er, 27.90.+b

I. INTRODUCTION

In the preceding paper [1] we briefly reviewed parity violation in the neutron-nucleus interaction. The early history is described in a monograph by Krupchitsky [2]. Following a suggestion by Sushkov and Flambaum [3], the Dubna group [4] observed very large parity-nonconserving (PNC) effects in the total cross section of epithermal neutrons on heavy nuclei.

The limitation of all previous measurements was the observation of only a single parity violation in a nuclide. We proposed the utilization of the intense neutron beam at the Los Alamos Neutron Scattering Center (LANSCE) to study parity violation for many resonances in a single nucleus and advocated a statistical approach to the extraction of a root-mean-square PNC matrix element M from the measured asymmetries for the p-wave resonances. The spirit of our approach was to utilize the complexity of the compound nuclear system, and by performing the measurements in a chaotic regime [5] to bypass the difficulties encountered in determining the nuclear wave functions for parity-violation studies in light nuclei [6]. Measurement of the helicity dependence of the neutron total cross section for ^{238}U yielded several nonzero PNC effects. After extension of the two-state approximation to include the contributions of many s-wave resonances, we used a statistical analysis to obtain a value for M and for the corresponding parity-violating spreading width Γ^{PV}. Using a prescription developed by French [7,8] to convert from the complicated compound nuclear system to the effective nucleon-nucleon system led to a reasonable value for the ratio of the symmetry-breaking strength to the symmetry-conserving part of the effective nucleon-nucleon interaction.

In the present experiment we report on results obtained at LANSCE in 1990 for ^{232}Th. A preliminary version of these results has been published [9]. We rely on the preceding paper [1] for much of the background, experimental method, and data reduction procedure. Here we emphasize differences between the two experiments. For the ^{232}Th experiment the target was cooled to liquid-nitrogen temperature which significantly reduced Doppler resonance broadening and extended the effective energy range available for study. We also employed a multilevel R-matrix code to analyze resonances which were not sufficiently well isolated to be treated as single levels. We analyzed 23 resonances in ^{232}Th at energies ranging from $E_n=8$ to 392 eV. Two resonances had asymmetries of order 10% (as large as any previously observed), and several resonances had parity violations with

*Present address: Los Alamos National Laboratory, Los Alamos, NM 87545.
†Present address: University of Pennsylvania, Philadelphia, PA 19104.
‡Present address: Indiana University, Bloomington, IN 47405.
§Present address: University of Washington, Seattle, WA 98195.

a relative significance of 2.4σ or greater. The longitudinal asymmetry had the same sign for all seven of these resonances, which contradicts the statistical assumptions employed in determination of the average PNC matrix element. The data (the experimental longitudinal asymmetries) were fit in two ways: with a purely statistical (fluctuating) term and as a sum of two terms [10]—a constant asymmetry and a fluctuating asymmetry.

The experimental method and the procedure to obtain the longitudinal asymmetries from the transmission spectra are briefly described in Secs. II and III. Differences from the experimental method described in the preceding paper are emphasized. The experimental data are presented in Sec. IV and the longitudinal asymmetries obtained. In Sec. V the data are interpreted with our standard statistical analysis. The issue of sign correlations is discussed in Sec. VI and a new model is used to obtain both the PNC matrix element M and a value for the constant term. The results are summarized in Sec. VII.

II. EXPERIMENTAL METHOD

A detailed description of the experimental procedure is given by Roberson *et al.* [11] and a summary is presented in the preceding paper [1]. Here we provide only a brief description.

The 800-MeV proton beam from the Los Alamos Meson Physics Facility (LAMPF) linac is injected into a proton storage ring (PSR) and the beam is compressed to a pulse width of $\sim$250 ns. The extracted proton beam strikes a tungsten target and neutrons are produced by the spallation process. The neutrons are moderated by water and collimated. Typical proton beam currents for the Th experiment were $\sim 60\ \mu$A.

The beam is polarized by selective attenuation through a cell of longitudinally polarized protons. The protons are polarized by dynamic nuclear polarization at 1-K temperature and 2-T magnetic field. The 2-T magnetic field is either parallel or antiparallel to the beam direction. The absolute polarization was determined by measurement of the parity violation at the 0.73-eV resonance in ^{139}La [12]. This method uses La as both target and analyzer, and directly measures the square of the parity violation. The resonance in ^{139}La is then measured during an experimental run using the "spin filter." Since the value of the parity violation for this resonance has been determined independently, this method provides an absolute value for the neutron polarization. The relative polarization of the beam is measured for each run by determining the proton polarization in the spin filter with NMR [11]. For the Th experiment the neutron polarization was about 27%.

Fast spin reversal was accomplished with a magnetic spin rotator or "spin flipper" [13], in which the neutron spin is reversed by a transverse field which has two possible directions. In one configuration there is a fixed longitudinal field which reverses sign at the midpoint of the spin flipper. To flip the neutron spin a transverse field is added to the longitudinal field. The transverse field sequence $\{0,+,-,0,+,0,0,-\}$ produces a spin sequence {parallel, antiparallel, A,P,A,P,P,A}. This eight-step sequence eliminates in first order the effect of transverse stray fields on the system and linear and quadratic time drifts in the detectors. The spin direction was reversed every ten seconds.

The target was a right circular cylinder of thorium metal, of thickness 0.093 atom/b (3.1 cm long), which contained trace impurities of tungsten. The target was located at the exit of the spin flipper. Doppler broadening is a major limitation in neutron experiments at these energies; the Doppler broadening is comparable to the natural width near one eV and at higher energies is larger than the natural width. In the simplest model the Doppler width Δ is proportional to $T^{1/2}$, where T is the temperature in K. Reducing the temperature from room temperature ($\sim$300 K) to liquid nitrogen temperature ($\sim$77 K) should reduce the Doppler width by a factor of about 2. A compact liquid nitrogen chiller was constructed to cool the sample [14]. Helmholtz coils were employed to extend a uniform axial magnetic guide field over the target region. Tests at room and liquid nitrogen temperatures indicated significant improvement when the target was cooled. In practice we could analyze data up to 400 eV, approximately 100 eV higher than in the ^{238}U experiment [1].

The neutrons were detected with a system of ^{6}Li-loaded glass detectors located at 56 m from the neutron source. Due to the very high count rates involved, the detectors were operated in current mode [15]. The neutron beam was monitored with a ^{3}He ionization chamber placed directly in front of the spin flipper. After each eight-step sequence the average neutron flux is determined and the data are accepted only if the average flux is within a predetermined range (normally $\pm 8\%$). Each step in the eight-step sequence lasted 200 neutron bursts (10 s). The sequence was then repeated 20 times and this collection of data (20 eight-step sequences) combined into a "run." These runs were then treated as the basic unit of data.

III. DETERMINATION OF LONGITUDINAL ASYMMETRIES

The parity-violating asymmetry P for a p-wave resonance is defined from

$$\sigma^{\pm}=\sigma_p(1\pm f_n P)\ , \tag{1}$$

where $\sigma^{\pm}$ is the resonance cross section for $+$ and $-$ helicity neutrons, σ_p the resonance part of the p-wave cross section, and f_n the neutron polarization. The neutron transmission yield at the detector is given by

$$\begin{aligned} N^{\pm}&=F(E_n)\exp\{-nt[\sigma_{\rm pot}+\sigma_p(1\pm f_n P)]\} \\ &=C(E_n)\exp[-nt\sigma_p(1\pm f_n P)]\ , \end{aligned} \tag{2}$$

where $F(E_n)$ is the neutron flux, E_n the neutron energy, $\sigma_{\rm pot}$ is the potential scattering cross section, $C(E_n)=F(E_n)\exp[-nt\sigma_{\rm pot}]$, n the number density of the ^{232}Th target nuclei, and t the thickness of the target. The final form for the transmission yield, after including Doppler broadening, expressing parameters directly in terms of time-of-flight (TOF) channel numbers, and al-

lowing for a slow energy dependence of the effective background, is

$$N^{\pm}=C^{\pm}\exp[-n\sigma'_{\max}\varphi(1\pm f_n p)] = \frac{N'(1\pm\alpha)}{K-K_s}\left[1+\sum_{i=1}^{5}\alpha_i\left[\frac{K-(K_b+K_e)/2}{1000}\right]^i\right] \times\exp[-n\sigma'_{\max}\varphi(1\pm f_n p)] , \quad (3)$$

where $C^{\pm}$ is the flux, $(\sigma'_{\max}\varphi)$ the Doppler-broadened p-wave resonance line shape, N' the normalization factor, K the TOF channel number, K_s the effective zero-TOF channel determined from the calibration, α the beam asymmetry in the two helicity states, and $[K_b,K_e]$ the range of channels under consideration. The polynomial in the square brackets accounts extremely well for effects which change slowly with energy, and usually provides an adequate description of the background even when the cross section is changing rapidly with energy. Thus this polynomial background simulates the s-wave background well for almost all of the resonances in ^{232}Th. The summed spectra were fit first to determine the general resonance parameters, and then each run fit following the procedure described by Zhu *et al.* [1]. It should be emphasized that this approach is a phenomenological fitting procedure, and that some of the fit parameters cannot be interpreted literally.

For resonances that could not be fit well by the single level fitting program, we used the multilevel, multichannel neutron resonance code SAMMY [16], which is based on the R-matrix formalism [17]. The minimum set of input parameters includes the target mass, the flight path length, the target thickness, and the quantum numbers l,J,π, and the resonance parameters E_n, Γ_γ, Γ_n for each resonance. Since the code SAMMY cannot fit the parity violating asymmetry directly, the following approach was adopted. The product $f_n P=(\sigma_p^+-\sigma_p^-)/(\sigma_p^++\sigma_p^-)$, where $\sigma_p^{\pm}$ is the p-wave cross section for $\pm$ helicity states. The Breit-Wigner cross section for the p-wave resonances is

$$\sigma_p=\pi\lambda\!\!\!^{-2}\Gamma_p^n\Gamma_p/[(E-E_p)^2+\Gamma_p^2/4] , \quad (4)$$

where Γ_p^n is the neutron partial width, Γ_p the total width, $\lambda\!\!\!^{-}$ the de Broglie wavelength in the center-of-mass (c.m.) system, and E the kinetic energy of the neutron-nucleus pair in the c.m. system. The resonance energy was determined from the experimental channel number and the calibration (see Sec. IV). For the resonances that required multilevel fits, the Doppler broadening is much larger than the natural width of the resonance. The broadening and background parameters were obtained from other nearby resonances, and the s-wave resonance parameters from the literature [18]. The capture width Γ_γ is nearly equal to the total width Γ. The p-wave resonance was fit (both + and − helicity spectra) with only the neutron width Γ_n varied and the combination $f_n P=(\Gamma_n^+-\Gamma_n^-)/(\Gamma_n^++\Gamma_n^-)$ obtained for each run. Since the program SAMMY fits neutron transmission spectra, not detector yields, the transmission for each run was calculated for each spin state, using a target-out run. The monitor counts for each spin state were used to obtain the correct normalization.

For the ^{232}Th data a multilevel analysis was required for only one p-wave resonance at $E_n=128.2$ eV, which strongly interfered with an s-wave resonance at $E_n=129.2$ eV. This analysis method was checked on a number of well-isolated resonances which had been analyzed with the single-level fitting procedure; the results of the two methods were in good agreement.

IV. EXPERIMENTAL DATA

The ^{232}Th production data were taken as 8192 channel spectra, with each channel having a TOF bin width of 200 ns. The effective energy window was 6–400 eV. This upper energy limit was approximately 100 eV higher than for the uranium data, with the increase presumably due to the cooled target which reduced the Doppler broadening. The neutron yields were sorted by helicity states and accepted or rejected depending on the range of fluctuations in the monitor counts. Each production run was carefully inspected before being accepted for final analysis. The final data set consisted of 355 runs.

As discussed in the preceding paper, there is background arising from γ rays in the neutron beam and/or scintillator afterglow, but this background does not affect the determination of the parity-violating asymmetry. The absolute neutron polarization was determined by measurement of the size of the parity violation at the 0.734-eV resonance in ^{139}La. This method uses La as both polarizer and analyzer—the double La experiment directly measures the square of the parity violation [12]. The neutron polarization for the thorium data is based on a series of ^{139}La measurements performed in the middle of the thorium measurements. The relative polarization of the neutrons was determined by measuring the proton polarization of the spin filter with NMR for each run. After the combination of $f_n P$ was determined for each run, the value of f_n was used to obtain the parity violation P.

The neutron time-of-flight $\mathrm{TOF}=7.23\times10^{-5}L/(E_n)^{1/2}$, where TOF is in seconds, L in meters, and E_n in eV. The transmission spectrum for ^{232}Th up to $E_n=400$ eV is shown in Fig. 1. The resonances in ^{232}Th up to 500

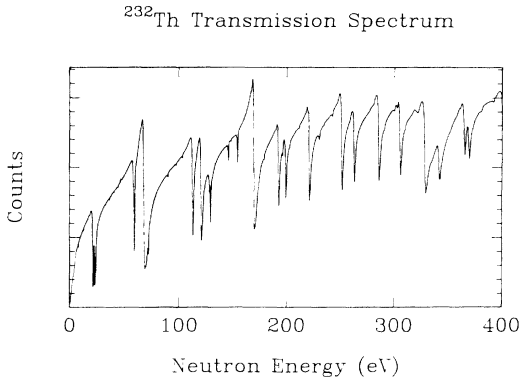

FIG. 1. The neutron transmission spectrum up to $E_n=400$ eV. The data are the sum of 355 runs used in the final analysis.

eV in the most recent evaluation [18] are listed in Table I. A detailed discussion of these resonance assignments is given below. The resonance energies in our data were determined by calibrating the peak channel number of many sharp resonances to their known energies.

Many experiments have been performed on ^{232}Th neutron resonances, including Olsen *et al.* [19], Corvi *et al.* [20], Ribon [21], and Forman [22]. The two most recent evaluations are by Bhat [23] and by Olsen [18]. There are several discrepancies between the two evaluations.

The 54.1-eV resonance was reported in only one previous measurement [22]; the neutron width was reported as 1.1×10^{-3} meV. As Fig. 2 shows, there is no evidence for this resonance in the present experiment. With the width reported by Forman *et al.* this resonance should be clearly visible in the present data. We conclude that the 54.1-eV resonance is not a ^{232}Th resonance.

The 112.1- and 117.8-eV resonances were reported in an unpublished dissertation [21] based on an experiment performed at Saclay. The neutron widths for the two resonances were reported as 3.9×10^{-3} and 2.0×10^{-3} meV, respectively. As shown in Fig. 2, there is no evidence in the current data for these two resonances. With the widths reported by Ribon for them, both resonances should have been clearly observed in the present data. We conclude that the 112.1 and 117.8-eV resonances are not ^{232}Th resonances.

The 192.6- and 391.8-eV resonances were assigned as *s* wave resonances in the Bhat evaluation. A capture γ-ray measurement by Corvi *et al.* [20] examined resonance decay to low-lying states in ^{233}Th. This γ-ray information was used to assign the resonances as *s*- wave or *p*- wave. Their analysis suggested that these two resonances are *p*-wave resonances.

The 219.5- and 309.5-eV resonances were assigned as *p*-wave resonances in the Bhat evaluation. Both are very small resonances initially assigned as *s* wave by Keyworth and Moore [24], who changed the assignments from *p*-wave to improve agreement with the Porter-Thomas reduced width distribution. In the present experiment, the energy resolution was not sufficient to permit analysis of these two weak resonances.

The resonances at 49.9, 232.1, 234.4, 242.2, 258.4, 272.8, 277.0, 335.2, and 352.0 eV are not listed in the Bhat evaluation. These resonances were reported by Forman [2] and/or Ribon [21]. All of these resonances are

TABLE I. ^{232}Th neutron resonance parameters.

E_n (eV)	l	$g\Gamma n$ (meV)	E_n (eV)	l	$g\Gamma_n$ (meV)
−22.2	0	6.266 5	232.25	1	0.013
−2.952	0	0.922 7	234.15	1	0.02
8.3505	1	0.000 275	242.41	1	0.041 9 2
13.124	1	0.000 209 5	251.65	0	31.78
21.806	0	2.06	258.43	1	0.009 885
23.464	0	3.85	263.23	0	22.22
36.991	1	0.000 940 7	272.76	1	0.019
38.191	1	0.000 575 8	276.97	1	0.035
41.032	1	0.000 586 8	285.91	0	31.03
47.044	1	0.001 531	290.58	1	0.062 69
49.875	1	0.000 483 3	299.84	1	0.041 52
54.156	1	0.001 1	302.68	1	0.141 5
58.771	1	0.008 976	305.62	0	28.88
59.519	0	3.80	304.47	0	0.056 41
64.499	1	0.000 694 0	321.83	1	0.044 34
69.232	0	43.2	329.11	0	74.48
90.167	1	0.006 145	335.23	1	0.034 66
98.069	1	0.003 976	338.34	1	0.053 61
103.66	1	0.005 54	342.00	0	38.89
112.05	1	0.003 939	352.00	1	0.077
113.03	0	13.13	361.35	1	0.099 99
117.82	1	0.001 97	365.36	0	26.06
120.87	0	22.51	369.49	0	25.71
128.20	1	0.068 57	380.72	0	0.122 9
129.19	0	3.381	391.83	0	0.144 5
145.86	1	0.089 19	401.10	1	11.12
148.05	1	0.010 35	402.92	0	0.105 9
154.36	1	0.198 6	411.99	1	0.211 4
167.17	1	0.018 65	421.03	1	0.502 5
170.39	0	61.25	427.34	1	0.019
178.96	1	0.029 4	454.47	0	1.227
192.72	0	16.9	459.20	1	0.065 48
196.25	1	0.081 7 2	462.77	0	64.07
199.40	0	10.24	466.41	1	0.106 8
202.72	1	0.0305	470.87	1	0.043 62
211.00	1	0.016 2 9	476.58	1	0.128 2
219.52	0	0.043 6 4	489.05	0	58.57
221.29	0	30.25			

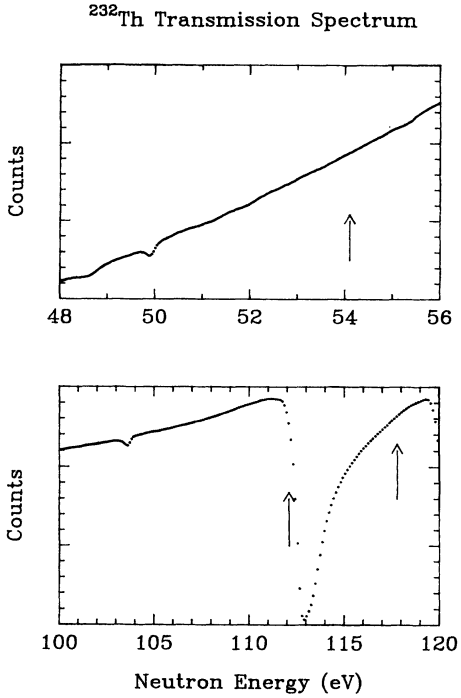

FIG. 2. Top: The ^{232}Th transmission spectrum in the vicinity of the resonance reported at 54.1 eV. The arrow shows the predicted location of the resonance. Bottom: The ^{232}Th transmission spectrum in the vicinity of the resonances reported at 112.1 and 117.8 eV. The arrows show the predicted locations of these resonances. Note that the ordinate zero is suppressed.

clearly observed in the present data. We conclude that they are all ^{232}Th resonances and probably are p wave.

For our analysis the parameters listed in the 1982 Olsen evaluation were used except for the resonances at 54.1, 112.1, and 117.8 eV. As noted above, the present data strongly indicate that these previously reported resonances are not ^{232}Th resonances.

In the effective energy range for this experiment (6 to 400 eV) there are 39 p-wave resonances listed in the 1982 Olsen evaluation, 36 after the three resonances discussed above are eliminated. All 36 are observed in the present experiment. Of these 36 p-wave resonances, values of the PNC asymmetry were obtained for 23 resonances. The 128.2-eV resonance was fit with the code SAMMY, while the other 22 resonances were fit with our single level code. Two of the remaining 13 resonances (at 47.0 and 321.8 eV) were not fit because they interfered with a contaminant resonance. The other 11 resonances were not fit because the energy resolution was insufficient to permit an accurate fit.

For the 22 resonances fit with the single-level program, we followed the procedure described in the preceding paper. We first determined the line-shape parameters which were assumed constant from run to run by fitting the summed spectrum. Then each run k was fit to determine the product of the parity violation P and the neutron polarization f_n—$(f_nP)_k$. An example is shown in the top part of Fig. 3. For each run k the polarization f_n was measured, and a value for P_k determined. The average parity-violating asymmetry is the weighted average of the individual P_k values. The weighting factors are the errors assigned to each value of f_nP by the fitting program. As discussed in the preceding paper, these errors should be reliable measures of the relative uncertainty in each P_k value, but may not be appropriate for the overall error in $\bar{P}$. We determined the error in $\bar{P}$ from the P_k distribution. The P_k values are histogrammed and the overall error δ determined from $\delta=\sigma/N^{1/2}$, where N is the number of runs and σ^2 is the variance of the P_k data set. The observed error σ reflects the statistics of a single run. Since δ is determined directly from the distribution, it should include all sources of error and be the most robust way to determine the overall error. A typical histogram is shown in the lower part of Fig. 3.

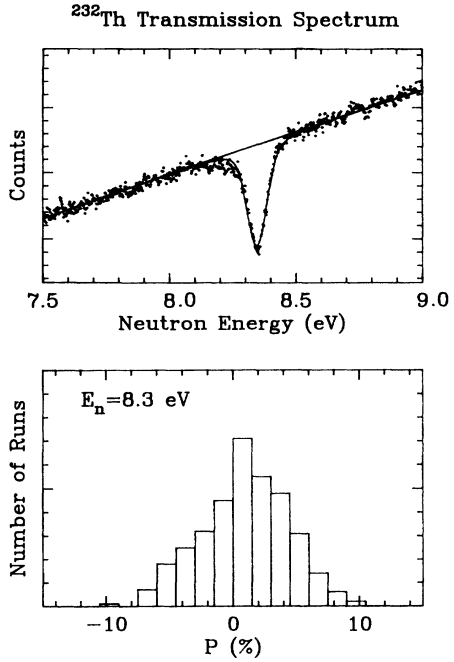

FIG. 3. Top: The transmission spectrum for a single run in the vicinity of the 8.35-eV resonance. The solid curves represent fits to the background and to the resonance with the single level program. The resonance parameters were obtained from the summed spectrum, and then with these resonance parameters held fixed, the longitudinal asymmetries P were obtained for each run. Note that the ordinate zero is suppressed. Bottom: Histogram of the asymmetry values for 355 runs at the 8.35-eV resonance.

For the one resonance that required a multilevel fit, the analysis procedure was essentially the same except for the difference in the method of determining the value of f_nP. A fit to the transmission spectrum for this resonance is shown in Fig. 4.

One additional correction is for the spin flipper [13]. The spin-preserving efficiency (s) is essentially 100%, while the spin-flipping efficiency (r) is less than 100% and is energy dependent [13]. The value of P extracted from our analysis is $P_{\text{code}}=P_{\text{true}}F_{\text{eff}}$, where the average spin-flipper efficiency is defined as $F_{\text{eff}}=(r+s)/2$. This correction is included in Table II, which lists the parity-violating asymmetries P. These asymmetries are plotted versus energy in Fig. 5.

The average raw off-resonance asymmetry was also examined for several cases. Using the summed spectra, the average asymmetry $\varepsilon=(N^+-N^-)/(N^++N^-)$ was al-

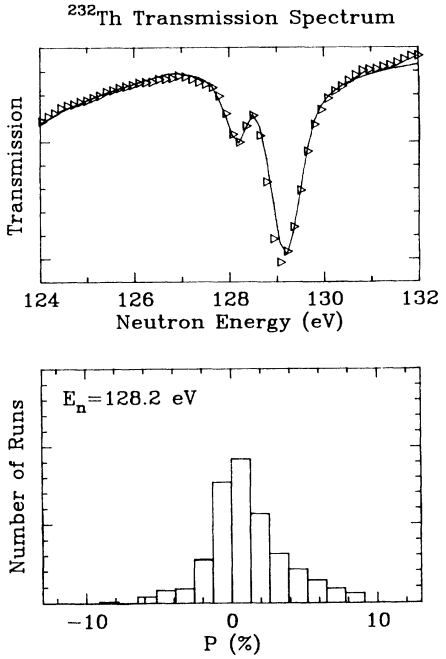

FIG. 4. Top: Fit to the p- and s-wave doublet ($E_p=128.2$ eV and $E_s=129.2$ eV) with the multilevel code SAMMY. Note that the ordinate zero is suppressed. Bottom: Histogram of the asymmetries for the 128.2 eV resonance.

TABLE II. Spin-flipper efficiencies, longitudinal analyzing powers, and relative significance of parity-violating asymmetries for p-wave neutron resonances in ^{232}Th.

E_n (eV)	F_{eff}	P_i (%)	$\lvert P_i\rvert/\delta_i$
8.3	0.98	1.48 ±0.25	5.9
13.1	1.00	0.74 ±0.62	1.2
37.0	0.99	2.46 ±0.97	2.5
38.2	0.99	10.88 ±2.27	4.8
41.0	0.99	−2.23 ±2.14	1.0
49.9	1.00	−1.08 ±2.99	0.4
64.5	1.00	9.78 ±2.08	4.7
90.2	0.98	−1.05 ±1.00	1.1
98.1	0.99	−0.01 ±1.38	0.0
103.7	1.00	−0.43 ±1.04	0.4
128.2	1.00	1.31 ±0.18	7.3
145.9	0.98	−0.03 ±0.22	0.1
148.1	0.97	−4.91 ±2.79	1.8
167.2	0.94	3.45 ±1.19	2.9
179.0	0.93	−1.47 ±1.28	1.1
196.2	0.91	1.10 ±0.46	2.4
202.7	0.91	2.17 ±1.43	1.5
211.0	0.90	1.76 ±1.85	1.0
242.3	0.90	−0.04 ±1.20	0.0
299.8	0.90	−1.56 ±1.68	0.9
302.7	0.90	−1.75 ±1.04	1.7
380.7	0.94	1.10 ±1.76	0.6
391.8	0.94	−0.67 ±1.62	0.4

ways consistent with zero, fluctuated in sign, and typically was of a factor $\times 10^{-5}$. The on-resonance asymmetries were typically a factor $\times 10^{-4}$.

We also analyzed a number of contaminant s-wave resonances. The results for four s-wave resonances which are due to ^{65}Cu, ^{156}Gd, ^{157}Gd, and ^{186}W are listed in Table III. Except for the 65 Cu 230 eV resonance, these resonances are intrinsically strong, but occur only in trace amounts, and thus are comparable in size to the ^{232}Th p-wave resonances of interest. The 230-eV ^{65}Cu resonance is a weak s-wave resonance, which is present due to the brass sleeve in which the thorium target was held. None of these s-wave resonances showed a statistically significant parity violation.

All available evidence indicates that in the present experiment, just as in the uranium experiment, the systematic errors are small compared with the experimental precision.

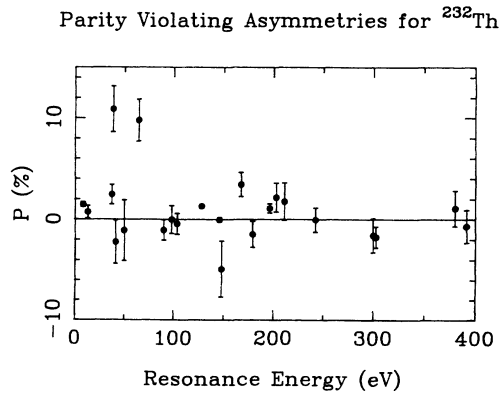

FIG. 5. The parity-violating longitudinal asymmetries P for 23 p-wave resonances in ^{232}Th.

TABLE III. Longitudinal analyzing powers for s-wave neutron resonances in ^{156}Gd, ^{157}Gd, ^{186}W, and ^{65}Cu.

E_n (eV)	P_i (%)
16.7 (^{157}Gd)	−0.08 ±1.27
18.8 (^{186}W)	−0.08 ±0.69
33.2 (^{156}Gd)	−1.39 ±2.52
230.0 (^{65}Cu)	0.45 ±0.66

V. ANALYSIS

The PNC asymmetries are listed in Table II and shown in Fig. 5. There are two asymmetries with values of 10.9% (38.2 eV) and 9.9% (64.5 eV); these are as large as the largest asymmetry previously observed (9.55% for the 0.734 eV resonance in ^{139}La). The transmission spectra for the two helicity states are shown in Fig. 6 for the 38.2-eV resonance. The parity violation is evident by inspection. There are seven PNC asymmetries with a statistical significance of 2.4σ or greater. This is the largest number of parity violations yet observed in a single nucleus and is consistent with the view that all p-wave resonances will display parity violation at some level. The relative significance P_i/δ_i is shown in Fig. 7. The most surprising result is that all seven of these statistically significant parity violations have the same sign. This is not consistent with the conventional statistical view in which the PNC longitudinal asymmetry P is a Gaussian random variable. In this section we neglect the sign correlations and apply the standard statistical theory. In Sec. VI we analyze the data with a new model which includes the sign correlation effect.

The PNC longitudinal asymmetry P has been obtained in the two-state model by many authors. In Zhu *et al.* [1] we outlined a derivation for P and reviewed physical

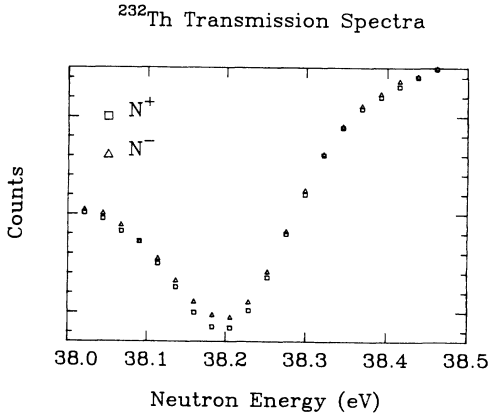

FIG. 6. The ^{232}Th transmission spectrum for the two helicity states − (triangles) and + (squares) in the vicinity of the 38.2-eV p-wave resonance. The parity violation is apparent by inspection. Note that the ordinate zero is suppressed.

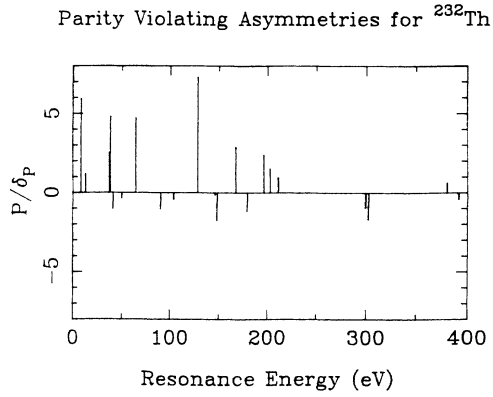

FIG. 7. Relative significance of PNC asymmetries in ^{232}Th.

arguments that predict very large PNC effects. In the two-level approximation P is

$$P=[2V/(E_s-E_p)][\Gamma_s^n/\Gamma_p^n]^{1/2}\ , \tag{5}$$

where the neutron widths are evaluated at the resonance energy E_p. The expression for P can be generalized to include the effects of all the s-wave resonances on a given p-wave resonance. If the s-wave resonances are labeled by j and the p-wave resonances by i, then

$$P_i=\sum_j A_{ij}V_{ij},\ A_{ij}=[2/(E_{sj}-E_\pi)][\Gamma_{sj}^n/\Gamma_\pi^n]^{1/2}\ . \tag{6}$$

For ^{232}Th all s-wave resonances up to 500 eV were included in the determination of A_{ij}. The A_{ij} values for a typical resonance (8.35 eV) are listed in Table IV.

The PNC matrix elements V_{ij} are assumed to be Gaussian distributed random variables with mean zero and variance M^2: $\langle V_{ij}\rangle=0$ and $\langle V_{ij}^2\rangle=M^2$. If the s-wave neutron widths, the p-wave neutron widths, and the energy spacings all are uncorrelated with the V_{ij}, then the observable P_i also is a Gaussian distributed random variable. The sum of Gaussian random variables is also a Gaussian random variable [25]. The ensemble averages of P_i and P_i^2 are then

$$\begin{aligned}\langle P_i\rangle&=\sum_j A_{ij}\langle V_{ij}\rangle=0\ ,\\ \langle P_i^2\rangle&=\left\langle\left[\sum_j A_{ij}V_{ij}\right]\left[\sum_{j'} A_{ij'}V_{ij'}\right]\right\rangle=A_i^2M^2\ ,\end{aligned} \tag{7}$$

where $A_i^2=\sum_j A_{ij}^2$. Including the experimental uncertainty δ_i leads to a variance $\langle P_i^2\rangle=A_i^2M^2+\delta_i^2$ for the distribution of P_i values. The probability of measuring a parity-violating asymmetry between P_i and P_i+dP_i is

$$\begin{aligned}F(P_i)dP_i&=\frac{1}{(2\pi\langle P_i^2\rangle)^{1/2}}\exp\left[-\frac{P_i^2}{2\langle P_i^2\rangle}\right]dP_i\\ &=\frac{1}{[2\pi(M^2+\delta_i^2/A_i^2)]^{1/2}}\exp\left[-\frac{(P_i/A_i)^2}{2(M^2+\delta_i^2/A_i^2)}\right]dP_i/A_i\\ &=\frac{1}{[2\pi(M^2+\delta_{Q_i}^2)]^{1/2}}\exp\left[-\frac{Q_i^2}{2(M^2+\delta_{Q_i}^2)}\right]dQ_i\ ,\end{aligned} \tag{8}$$

where $Q_i=P_i/A_i$ and $\delta_{Q_i}=\delta_i/A_i$. The new variable Q also has the property that its mean is zero and its variance M^2: $\langle Q_i\rangle=0$ and $\langle Q_i^2\rangle=M^2$. This key result implies that if the A_{ij} are known, the value of the root-mean-square matrix element M can be determined directly from the measured values P_i. The values of P, A, and Q are listed in Table V.

The spins of most of the p-wave resonances are unknown. We therefore adopt a statistical approach, and assume that the angular momentum values of the p-wave resonances are unknown. For low spins the level density is approximately proportional to $(2J+1)$. We assume a $\frac{1}{3}$ probability for the p-wave resonances to have $J=\frac{1}{2}$ and a $\frac{2}{3}$ probability to have $J=\frac{3}{2}$. The probability for a resonance to show a parity violating asymmetry between P_i and P_i+dP_i is then

$$F(P_i)dP_i=\left\{\frac{1}{3}\frac{1}{[2\pi(M^2+\delta_{Q_i}^2)]^{1/2}}\exp\left[-\frac{Q_i^2}{2(M^2+\delta_{Q_i}^2)}\right]+\frac{2}{3}\frac{1}{(2\pi\delta_{Q_i}^2)^{1/2}}\exp\left[-\frac{Q_i^2}{2\delta_{Q_i}^2}\right]\right\}. \tag{9}$$

TABLE IV. The A_{ij} coefficients for the p-wave resonance at $E_i=8.35$ eV.

E_j (eV)	A_{ij} (eV^{-1})[a]	E_j (eV)	A_{ij} (eV^{-1})[a]
−22.2	7.74	251.65	1.19
−2.952	13.33	263.23	0.94
21.806	10.12	285.91	1.00
23.464	12.09	305.62	0.89
59.519	2.81	309.47	0.04
69.232	7.67	329.11	1.30
113.03	2.18	342.00	0.89
120.87	2.61	365.36	0.67
129.19	0.93	369.49	0.66
154.36	0.18	401.10	0.39
170.39	2.74	402.92	0.04
192.72	1.23	421.03	0.08
199.40	0.91	454.47	0.11
219.52	0.05	462.77	0.78
221.29	1.37	489.05	0.69

[a]The parity violation for the ith p-wave resonance is $P_i=\sum A_{ij}V_{ij}$. For the 8.35 eV resonance $(\sum_j A_{ij}^2)^{1/2}=24.21$ eV^{-1}.

The likelihood function is the joint probability of all 23 p-wave resonances and can be written as

$$L(M)=N_0\prod_{i=1}^{23}\left\{\frac{1}{3}\frac{1}{[2\pi(M^2+\delta_{Q_i}^2)]^{1/2}}\exp\left[-\frac{Q_i^2}{2(M^2+\delta_{Q_i}^2)}\right]+\frac{2}{3}\frac{1}{(2\pi\delta_{Q_i}^2)^{1/2}}\exp\left[-\frac{Q_i^2}{2\delta_{Q_i}^2}\right]\right\}, \tag{10}$$

where N_0 normalizes the likelihood function as $\int_0^{M_{\max}}L(M)dM=1$. We chose $M_{\max}=10$ meV for the normalization. The results were insensitive to the ratio of $J=\frac{1}{2}$ and $\frac{3}{2}$ states.

The likelihood function is shown as a smooth curve in Fig. 8. The most compact region of 68% confidence level is represented by the shaded area. The most likely value of M is

$$M=1.39^{+0.55}_{-0.38}\text{ meV}. \tag{11}$$

We assume that the $p_{1/2}$ and $s_{1/2}$ level spacings are the same, and take the s-wave level spacing from the literature [18]. Then with $M=1.39$ meV and the level spacing $D=16.4$ eV, the parity-violating spreading width Γ^{PV} is

$$\Gamma^{PV}=2\pi M^2/D=7.4^{+8.2}_{-3.8}\times10^{-7}\text{ eV}. \tag{12}$$

In the simplest picture [7,8] the ratio of the symmetry-breaking strength to the symmetry conserving strength is given by

$$|\alpha_p|=[\Gamma^{PV}/(2\pi\times10^5\text{ eV})]^{1/2}\approx11\times10^{-7}. \tag{13}$$

The value for $|\alpha_p|$ is qualitatively reasonable, since one expects that α_p should be a factor $\times10^{-7}$. Johnson *et al.* [26] discuss the procedure for obtaining α_p from the experimental value of the PNC matrix element. However, as noted above, our analysis neglects the existence of sign correlations. This issue is considered in the next section.

TABLE V. Parity violations for p-wave neutron resonances in ^{232}Th.

E_n (eV)	P_i (%)	$(\sum_j A_{ij}^2)^{1/2}$ (eV^{-1})	Q_i (meV)
8.3	1.48 ±0.25	24.20	0.61 ±0.10
13.1	0.74 ±0.62	36.40	0.20 ±0.17
37.0	2.46 ±0.97	19.12	1.28 ±0.51
38.2	10.88 ±2.27	24.24	4.49 ±0.94
41.0	−2.23 ±2.14	24.40	−0.91 ±0.88
49.9	−1.08 ±2.99	36.53	−0.30 ±0.82
64.5	9.78 ±2.08	108.6	0.90 ±0.19
90.2	−1.05 ±1.00	10.83	−0.97 ±0.92
98.1	−0.01 ±1.38	13.54	−0.01 ±1.02
103.7	−0.43 ±1.04	14.42	−0.30 ±0.72
128.2	1.31 ±0.18	15.26	0.86 ±0.12
145.9	−0.03 ±0.22	2.99	−0.10 ±0.74
148.1	−4.91 ±2.79	9.07	−5.42 ±3.08
167.2	3.45 ±1.19	35.68	0.97 ±0.33
179.0	−1.47 ±1.28	11.77	−1.25 ±1.09
196.2	1.10 ±0.46	11.23	0.39 ±0.41
202.7	2.17 ±1.43	13.07	1.66 ±1.09
211.0	1.76 ±1.85	11.13	1.58 ±1.66
242.3	−0.04 ±1.20	7.30	−0.05 ±1.64
299.8	−1.56 ±1.68	10.70	−1.45 ±1.57
302.7	−1.75 ±1.04	10.13	−1.73 ±1.03
380.7	1.10 ±1.76	3.78	2.91 ±4.66
391.8	−0.67 ±1.62	2.85	−2.35 ±5.68

VI. SIGN CORRELATIONS

The present data are not consistent with the assumption of independent variables randomly distributed in sign. Figure 7 shows the statistical significance P_i/δ_i for the resonances studied in ^{232}Th. All seven asymmetries with statistical significance $>2.4\sigma$ have positive sign. The chance of obtaining the same sign for seven out of seven randomly distributed quantities is 1.6%. Assuming that these seven resonances are $p_{1/2}$, the Q's are sampled from Gaussians of width $M^2+\sigma_{Q_i}^2$. Then $Q_{\text{ave}}=1.31\pm0.55$, or 2.4σ different from zero.

The signs of the other known PNC asymmetries also can be considered, since all are known relative to the sign of the resonance in ^{139}La, the sign of which has been confirmed by Masuda *et al.* [27] and by our group [12]. Five of the seven $>2\sigma$ effects (other than in ^{232}Th) are also positive. There are results from Alfimenkov *et al.* [4] for ^{81}Br (0.88 eV), ^{117}Sn (1.33 eV), and ^{139}La (0.73 eV) and from our previous work [1,28] for ^{238}U (63.5 and 83.7 eV). We have confirmed the sign of the ^{81}Br [29] and the ^{117}Sn effects [30]. The only published negative values are a 7σ effect in ^{111}Cd (4.53 eV) [4] and a 2σ effect in ^{238}U (89.2 eV) [1]. The probability of 12 of 14 randomly distributed quantities having the same sign is 1.1%. There is a preliminary report of another negative effect for ^{113}Cd (7.0 eV) [31].

Although more data on these sign correlations are required to definitively establish the effect, here we assume that the sign correlation is established. There are now several approaches which attempt to explain the sign

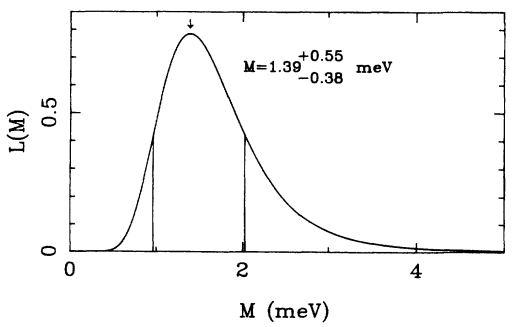

FIG. 8. Likelihood function of the 23 p-wave resonances in ^{232}Th. The arrow indicates the value of $M=1.39$ meV, while the vertical lines indicate the range of the 68% confidence level.

correlation by Bowman *et al.* [10], Flambaum [32], Auerbach [33], Weidenmüller [34], and Koonin [35]. Since the observed asymmetries appear to have a nonzero average value and also show appreciable fluctuations, a realistic analysis requires both a constant term and a fluctuating term.

Here we adopt the approach followed by Bowman *et al.* [10]. They express the asymmetry as the sum of two terms: a constant asymmetry dominated by admixtures of distant levels and a fluctuating asymmetry dominated by admixtures of nearby compound nuclear resonances. The constant asymmetry involves single-particle transition amplitudes of the parity-violating interaction, while the fluctuating asymmetry retains its statistical character. In the notation of the present paper the result is

$$P_i = 2[\sum_j V_{ij}/(E_j - E_i)](\Gamma_j^n/\Gamma_i^n)^{1/2} + B[(1\text{ eV})/E]^{1/2} , \tag{14}$$

where E is in eV. The set of quantities V_{ij}, Γ_i, Γ_j can be treated as independent random variables and the first (fluctuating) term has average value zero. The energy dependence of $(\Gamma_j^n/\Gamma_i^n)^{1/2}$ is $(kR)^{-1}$ or $E^{-1/2}$. Expressing the constant term relative to the value at $E_n = 1$ eV gives the convenient result that the ratio of the fluctuating and constant terms does not depend on energy.

In order to apply this analysis to the thorium data, the maximum-likelihood analysis must be modified to include B as well as M. In addition, one must evaluate the probability q that the resonances analyzed actually have angular momentum $J = \frac{1}{2}$. In the analysis of the uranium data, the PNC matrix element M was found to be insensitive to q, which was taken to be $\frac{1}{3}$. However, in the two-dimensional likelihood analysis, B depends on the value of q because $p_{1/2}$ resonances are on average twice as strong as $p_{3/2}$ resonances and because we do not observe all of the resonances. We estimate q by considering the fraction f of all p-wave resonances that are analyzed. Up to 400 eV one expects $\sim 3\Delta E/D = (3\times 400)/16.4 = 73$ p-wave resonances. Since we analyzed only 23 resonances, $f = 0.32$. This determines the minimum width parameter $u = (\gamma_{1/2})_{\min}/\langle\gamma_{1/2}\rangle$, where $(\gamma_{1/2})_{\min}$ is the weakest $p_{1/2}$ partial width amplitude that we can detect:

$$f = [\operatorname{erfc}(u/\sqrt{2}) + 2\operatorname{erfc}(u)]/3 . \tag{15}$$

Knowing u in turn determines the probability q that the p-wave resonances we observe have $J = \frac{1}{2}$:

$$q = \operatorname{erfc}(u/\sqrt{2})/3f . \tag{16}$$

The experimental value $f = 0.32$ gives $q = 0.45$. With this value for q, analysis of the thorium PNC data yields $B = (7.7\pm 6.2)\%$ and $M = 1.2^{+0.5}_{-0.4}$ meV. If half of the levels were observed and analyzed ($f = 0.5$ and $q = 0.40$), then the two-dimensional likelihood analysis gives $b = (8.3\pm 6.4)\%$ and M is unchanged.

It is important to note that the value of M is not extremely sensitive to q and B. The value of M obtained from the two-term expression is about 15% smaller than that obtained with only a fluctuating term. It seems plausible that the phenomenological fitting equation will have the same form independent of the particular model for the sign correlations. From the new value of M and the average level spacing for $J = \frac{1}{2}$ levels in ^{233}Th, the parity-violating spreading width $\Gamma^{PV} = 2\pi M^2/D = 5.5^{+5.6}_{-3.0} \times 10^{-7}$ eV. The value for Γ^{PV} (and therefore α_p) is somewhat higher than for ^{238}U, but within experimental uncertainties.

VII. SUMMARY

We have obtained the PNC longitudinal analyzing powers for 23 p-wave resonances in ^{232}Th. Seven resonances show parity violations of greater than 2.4σ statistical significance—the largest sample measured for a single nuclide. The most surprising result is that all seven of these statistically significant parity violations have the same sign. This requires a generalization of the purely statistical approach that we originally adopted. The asymmetry data were analyzed in two ways: with a purely statistical term and as a sum of two terms—a constant asymmetry and a fluctuating asymmetry. The values for the PNC matrix element M determined by the two methods were $M_{Th} = 1.4$ and 1.2 meV. These values for M are qualitatively consistent with our previous determination of M in ^{238}U ($M_U = 0.6$ meV).

There are a number of unresolved issues. The mechanism for the parity violation needs to be clarified. More experimental data are required to definitively establish the sign correlations. Several theoretical interpretations have been proposed. It would be valuable to have concrete predictions from these models (for example, concerning mass dependence, sign and magnitude of the correlations, and off-resonance behavior). It is very important to obtain more data in the $A = 230$–240 mass region in order to determine M more precisely. It is also important to study other mass regions, for example, in the vicinity of the $3p$ size resonance near $A = 100$. The experimental goal is to determine the magnitude of B and M more precisely, and to determine their mass dependence. With improved experimental results, the questions concerning the reaction mechanism should be resolved, and more precise values obtained for the PNC matrix element M. Extension of the theoretical approach proposed by Johnson *et al.* [26] should provide a connection between the observed PNC matrix element and the effective nucleon-nucleon interaction.

Improved experimental facilities will enhance these experimental efforts. A new system with an improved neutron spin-polarizer and detection system will be available in the near future. These first few results for ^{238}U and ^{232}Th are already important, in that they demonstrate the value of studying symmetry breaking in the chaotic compound nucleus, where one can bypass many of the difficulties encountered in light nuclei. The study of the neutron-nucleus PNC interaction appears to have a promising future.

ACKNOWLEDGMENTS

The authors would like to thank E. D. Davis, G. T. Garvey, A.C. Hayes, and H. A. Weidenmüller for valuable discussions. This work was supported in part by the U.S. Department of Energy, Office of High Energy and Nuclear Physics, under Grants No. DE-FG05-88-ER40441 and No. DE-FG05-91-ER40619 and by the U.S. Department of Energy, Office of Energy Research, under Contract No. W-7405-ENG-36.

[1] X. Zhu *et al.*, Phys. Rev. C **46**, 768 (1992), the preceding paper.
[2] P. A. Krupchitsky, *Fundamental Research with Polarized Slow Neutrons* (Springer Verlag, Berlin, 1987).
[3] O. P. Sushkov and V. V. Flambaum, Yad. Fiz. **32**, 377 (1980) [JETP Lett. **32**, 352 (1980)].
[4] V. P. Alfimenkov, S. Borzakov, Vo Van Thuan, Yu. D. Mareev, L. B. Pikelner, A. S. Khrykin, and E. I. Sharapov, Nucl. Phys. **A398**, 93 (1983).
[5] O. Bohigas and H. A. Weidenmüller, Annu. Rev. Part. Sci. **38**, 421 (1988).
[6] E. G. Adelberger and W. C. Haxton, Annu. Rev. Nucl. Part. Sci. **35**, 501 (1988).
[7] J. B. French, V. K. B. Kota, A. Pandey, and S. Tomsovic, Ann. Phys. (N.Y.) **181**, 198 (1988).
[8] J. B. French, A. Pandey, and J. Smith, in *Tests of Time Reversal Invariance in Neutron Physics,* edited by N. R. Roberson, C. R. Gould, and J. D. Bowman (World Scientific, Singapore, 1987), p. 80.
[9] C. M. Frankle *et al.*, Phys. Rev. Lett. **67**, 564 (1991).
[10] J. D. Bowman *et al.*, Phys. Rev. Lett. **68**, 780 (1992).
[11] N. R. Roberson *et al.*, Nucl. Instrum. Methods (to be published).
[12] V. W. Yuan *et al.*, Phys. Rev. C **44**, 2187 (1991).
[13] J. D. Bowman and W. B. Tippens, Nucl. Instrum. Methods (to be published).
[14] C. M. Frankle, Ph.D. dissertation, North Carolina State University, 1991.
[15] J. D. Bowman, J. J. Szymanski, V. W. Yuan, C. D. Bowman, A. Silverman, and X. Zhu, Nucl. Instrum. Methods **A297**, 183 (1990).
[16] N. M. Larson, Oak Ridge National Laboratory Report No. ORNL/TM-9179/R2 (1989).
[17] A. M. Lane and R. G. Thomas, Rev. Mod. Phys. **30**, 257 (1958).
[18] D. K. Olsen, Oak Ridge National Laboratory Report No. ORNL/TM-8056 (1982).
[19] D. K. Olsen, R. W. Ingle, and J. L. Portney, Nucl. Sci. Eng. **82**, 289 (1982).
[20] F. Corvi, G. Pasquariello, and T. van der Veer, International Conference on Neutron Physics and Nuclear Data, Harwell, 1978 (OECD Nuclear Energy Agency), p. 712.
[21] P. Ribon, Ph.D. dissertation, University of Paris, 1969.
[22] L. Forman, A. D. Schelberg, J. H. Warren, M. V. Harlow, H. A. Grench, and N. W. Glass, Proceedings of the Third Conference on Neutron Cross Sections and Technology, Knoxville, 1971, CONF-710301 (National Technical Information Service), p. 735.
[23] M. L. Bhat, Brookhaven National Laboratory Report No. BNL-NCS-17541 (1979).
[24] G. A. Keyworth and M. S. Moore, International Conference on Neutron Physics and Nuclear Data, Harwell, 1978 (OECD Nuclear Energy Agency), p. 241.
[25] W. T. Eadie, D. Drijard, F. E. James, M. Roos, and B. Sadoulet, *Statistical Methods in Experimental Physics* (North Holland, Amsterdam, 1971).
[26] M. B. Johnson, J. D. Bowman, and S. H. Yoo, Phys. Rev. Lett. **76**, 310 (1991).
[27] Y. Masuda, T. Adachi, A. Masaike, and K. Morimoto, Nucl. Phys. **A504**, 269 (1989).
[28] J. D. Bowman *et al.*, Phys. Rev. Lett. **65**, 1721 (1990).
[29] C. M. Frankle *et al.*, Phys. Rev. C (to be published).
[30] E. I. Sharapov, S. A. Wender, H. Postma, S. J. Seestrom, C. R. Gould, O. A. Wasson, Yu. P. Popov, and C. D. Bowman, in *Capture Gamma-Ray Spectroscopy,* edited R. W. Hoff (AIP, New York, 1991) p. 756.
[31] V. P. Alfimenkov, Yu. D. Mareev, L. B. Pikelner, V. R. Skoy, and V. N. Shvetsov, Yad. Fiz. **54**, 1489 (1991).
[32] V. V. Flambaum, Phys. Rev. C **45**, 437 (1992).
[33] N. Auerbach, Phys. Rev. C **45**, 514 (1992).
[34] H. A. Weidenmüller (private communication).
[35] S. E. Koonin (private communication).